Effect of the Trimethylsilyl Substituent on the Reactivity of Permethyltitanocene

Jiří Pinkas,[†] Lenka Lukešová,[†] Róbert Gyepes,[‡] Ivana Císařová,[‡] Peter Lönnecke,[§] Jiří Kubišta,[†] Michal Horáček,[†] and Karel Mach*[,†]

J. Heyrovský Institute of Physical Chemistry of Academy of Sciences of the Czech Republic, v.v.i., Dolejškova 3, 182 23 Prague 8, Czech Republic, Department of Inorganic Chemistry, Faculty of Science, Charles University, Hlavova 2030, 128 40 Prague 2, Czech Republic, and Institut für Anorganische Chemie, Universität Leipzig, Johannisallee 29, 04103 Leipzig, Germany

Received February 21, 2007

The presence of a trimethylsilyl substituent in place of one of the methyl groups of each of the cyclopentadienyl ligands of decamethyltitanocene enhances the thermal stability of the resulting complex, $[Ti^{II}\{\eta^5\text{-}C_5Me_4(SiMe_3)\}_2]$ (**1**), and controls the products formed in thermolysis of its methyl derivatives. Titanocene **1** was found to be stable in toluene solution up to 90 °C, while under vacuum at 140 °C it liberated hydrogen to give the asymmetrical doubly tucked-in titanocene $[Ti^{II}\{\eta^3{:}\eta^4\text{-}C_5Me_2(SiMe_3)(CH_2)_2\}\text{-}\{\eta^5\text{-}C_5Me_4(SiMe_3)\}]$ (**3**). The mono- and dimethyl derivatives of **1**, the complexes $[Ti^{III}Me\{\eta^5\text{-}C_5Me_4\text{-}(SiMe_3)\}_2]$ (**5**) and $[Ti^{IV}Me_2\{\eta^5\text{-}C_5Me_4(SiMe_3)\}_2]$ (**6**), undergo thermolysis at lower temperature than do the corresponding permethyltitanocene derivatives and eliminate hydrogen from their trimethylsilyl group. Thus, the known $[Ti^{III}\{\eta^5{:}\eta^1\text{-}C_5Me_4(SiMe_2CH_2)\}\{\eta^5\text{-}C_5Me_4(SiMe_3)\}]$ (**4**) was obtained from **5**, and compound **6** afforded $[Ti^{II}\{\eta^6{:}\eta^1\text{-}C_5Me_3(CH_2)(SiMe_2CH_2)\}\{\eta^5\text{-}C_5Me_4(SiMe_3)\}]$ (**7**) at only 90 °C, both with liberation of methane. Crystal structures of **3**, **5**, and **7** were determined. DFT calculations for titanocene **1** revealed that the metal−cyclopentadienyl bonding is accomplished via a three-center−four-electron orbital interaction. An auxiliary long-range Si−C bond interaction with the Ti center was also established, providing a reason for the enhanced thermal stability of **1**. The molecular orbitals participating in the exo methylene−titanium bonds for **3** and **7** are also three-centered and are compatible with the assignment of their activated ligands to $\eta^3{:}\eta^4$-allyldiene and η^6-fulvene structures, respectively. Qualitatively, the much higher thermal stability of **3** and **7** compared to that of **1** is due to the exploitation of four d orbitals in the bonding molecular orbitals for **3** and **7** versus only two d orbitals for **1**.

Introduction

The chemistry of decamethyltitanocene $[Ti(\eta^5\text{-}C_5Me_5)_2]$ (I) is well understood, although it is limited by the thermal instability of this complex, which inherently forms an equilibrium with its single tucked-in (aka η^6-fulvene) hydride $[TiH\text{-}\{\eta^6\text{-}C_5Me_4(CH_2)\}(\eta^5\text{-}C_5Me_5)]$ (II) at ambient temperatures. When it is sublimed at 80 °C, the titanocene I/II eliminates hydrogen to give $[Ti^{III}\{\eta^5{:}\eta^1\text{-}C_5Me_4(CH_2)\}(\eta^5\text{-}C_5Me_5)]$ (III).[1a] The Ti−methyl derivatives of I are stable at ambient temperature; however, when heated they cleanly eliminate methane. The monomethyl species $[TiMe(\eta^5\text{-}C_5Me_5)_2]$ affords III at 110 °C,[2] and the dimethyl species $[TiMe_2(\eta^5\text{-}C_5Me_5)_2]$ gives the single tucked-in complex $[TiMe\{\eta^6\text{-}C_5Me_4(CH_2)\}(\eta^5\text{-}C_5Me_5)]$ (IV) at 130 °C.[1b−d] Compounds III and IV then at 150 °C give rise to the double tucked-in (aka $\eta^3{:}\eta^4$-allyldiene) species $[Ti\{\eta^3{:}\eta^4\text{-}C_5Me_3(CH_2)_2\}(\eta^5\text{-}C_5Me_5)]$ (V), albeit in moderate yield (see Scheme 1).[2a] It is of interest that compound V can be obtained quantitatively by thermolysis of the bis-(trimethylsilyl)ethyne (btmse) complex $[Ti(\eta^2\text{-btmse})(\eta^5\text{-}C_5\text{-}Me_5)_2]$ with the elimination of 1,2-bis(trimethylsilyl)ethene (trans ≫ cis).[3]

The structure and bonding in compounds I−V are known to various extents. The effective magnetic moment of I, $\mu = 2.60 \pm 0.01\ \mu_B$ at 25 °C (lower than the theoretical value of 2.83 μ_B) and the large paramagnetic broadening of the ^{1}H NMR resonances of I and their temperature-dependent paramagnetic shifts, as well as the absence of EPR signals, show that the d^2 Ti(II) ion forms a poorly defined triplet state.[1a] Compound III contains a paramagnetic d^1 Ti(III) ion, as evidenced by its EPR spectrum ($g = 1.952$, $\Delta H = 7$ mT), electronic absorption band at λ_{max} 550 nm, and lowest vertical ionization energy of 5.54 eV in He I and He II photoelectron spectra (intensity ratio He II/He I = 1.00) that is typical for a SOMO d(Ti).[4] The fulvene representation for IV and the allyldiene for V as shown in Scheme 1 are supported by ^{1}H NMR spectra showing low $^2J_{HH} = 4$ Hz values for the diastereotopic $=CH_2$ hydrogens and by ^{13}C NMR resonances of $=CH_2$: δ 73.9 and $^1J_{CH} = 150$ Hz for

* To whom correspondence should be addressed. E-mail: mach@jh-inst.cas.cz.

† Academy of Sciences of the Czech Republic.

‡ Charles University.

§ Universität Leipzig.

(1) (a) Bercaw, J. E. *J. Am. Chem. Soc.* **1974**, *96*, 5087−5095. (b) Bercaw, J. E.; Brintzinger, H. H. *J. Am. Chem. Soc.* **1971**, *93*, 2045−2046. (c) Bercaw, J. E.; Marvich, R. H.; Bell, L. G.; Brintzinger, H. H. *J. Am. Chem. Soc.* **1972**, *94*, 1219−1238. (d) McDade, C.; Green, J. C.; Bercaw, J. E. *Organometallics* **1982**, *1*, 1629−1634.

(2) (a) Pattiasina, J. W.; Hissink, C. E.; de Boer, J. L.; Meetsma, A.; Teuben, J. H.; Spek, A. L. *J. Am. Chem. Soc.* **1985**, *107*, 7758−7759. (b) Luinstra, G. A.; Teuben, J. H. *J. Am. Chem. Soc.* **1992**, *114*, 3361−3367.

(3) Varga, V.; Mach, K.; Polášek, M.; Sedmera, P.; Hiller, J.; Thewalt, U.; Troyanov, S. I. *J. Organomet. Chem.* **1996**, *506*, 241−251.

(4) (a) Vondrák, T.; Mach, K.; Varga, V.; Terpstra, A. *J. Organomet. Chem.* **1992**, *425*, 27−39. (b) Mach, K.; Varga, V.; Hanuš, V.; Sedmera, P. *J. Organomet. Chem.* **1991**, *415*, 87−95.

10.1021/om070159l CCC: $37.00
Publication on Web 05/25/2007

Scheme 1

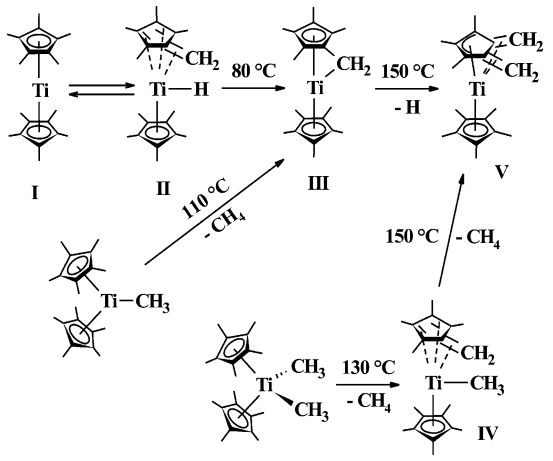

IV[1d] and δ 67.6 and $^1J_{CH}$ = 160 Hz for V.[2a] An olefinic C−H stretching IR vibration was observed at 3040 cm^{-1} for IV[1d] and at 3020 cm^{-1} for V.[2a] The lowest ionization energy bands in He I photoelectron spectra at 6.50 eV for IV and 6.55 eV for V cannot be assigned to a d(Ti) orbital. Extended Hückel MO calculations led to the conclusion that both IV and V can be considered to be d^0 complexes where, however, the metal d orbitals strongly interact with π orbitals to give stabilized HOMO orbitals.[4a] The turquoise IV and blue V show electronic absorption bands at 605 and 590 nm, respectively,[4b] in tentative agreement with the above EHT calculations. Compound II, observed only in a mixture with I, was characterized by its green color and a narrow resonance in its ^{1}H NMR spectrum similar to that of IV. It was therefore tentatively assigned as a hydride analogue of IV.[1a]

In contrast to the thermally unstable permethyltitanocene I, the silicon-containing titanocenes [Ti{η^5-C$_5$Me$_4$(SiR$_2$R′)}$_2$] (R = Me, R′= *t*-Bu;[5a] R = R′= Me;[5b] R = Me, R′= Ph; R = Ph, R′= Me; R = Me, R′= CH$_2$CH$_2$Ph;[5c] R = Me, R′ = *i*-Pr[5d]) appeared to be stable at room temperature under an inert atmosphere. The stability of bis(η^5-tetramethyl(trimethylsilyl)-cyclopentadienyl)titanium(II) (**1**) in particular is known to be surprisingly high, since it was cleanly prepared by thermolysis of [Ti(η^2-btmse){η^5-C$_5$Me$_4$(SiMe$_3$)}$_2$] (**2**) at 80 °C under vacuum.[5b] Unlike [Ti(η^2-btmse)(η^5-C$_5$Me$_5$)$_2$], which can be prepared from [TiCl$_2$(η^5-C$_5$Me$_5$)$_2$] by reduction with an excess of magnesium in the presence of an excess of btmse at elevated temperature,[3] compound **2** reacts further with magnesium even at −5 °C. At 60 °C, the temperature which is advantageously used to produce the titanocene−btmse complexes from the titanocene dichlorides in the presence of btmse,[3,6] the reaction afforded instead of the btmse complex the intramolecular silylmethylene-bridged paramagnetic complex [Ti^{III}{η^5:η^1-C$_5$-Me$_4$(SiMe$_2$CH$_2$)}{η^5-C$_5$Me$_4$(SiMe$_3$)}] (**4**) as the main product (see Chart 1). In the absence of btmse, the reduction afforded mainly the trinuclear paramagnetic complex [{{η^5-C$_5$Me$_4$SiMe$_2$-

Chart 1

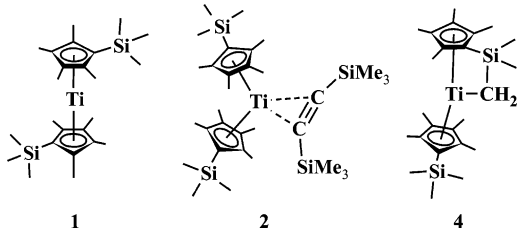

(μ-CH$_2$(*Mg*,*Mg*))}{η^5-C$_5$Me$_4$(SiMe$_3$)}Ti^{III}(μ-H)$_2$Mg-(THF)}$_2$].[7] Reactions leading to both of the main products have not been elucidated; however, the exclusive activation of the trimethylsilyl groups is their common feature.

In this work we report the products arising from thermolysis of titanocene **1** and its mono- and dimethyl derivatives [Ti^{III}-Me(η^5-C$_5$Me$_4$(SiMe$_3$)$_2$] (**5**) and [TiMe$_2${η^5-C$_5$Me$_4$(SiMe$_3$)}$_2$] (**6**), respectively, with the aim of finding out whether activation of cyclopentadienyl methyl groups can compete with activation of the trimethylsilyl groups in the thermolytic elimination of hydrogen or methane. Reasons for the high thermal stability of **1** and for the thermolytic products will be sought in MO bonding modes as obtained from DFT calculations.

Results and Discussion

The thermolysis of titanocene **1** or its btmse complex **2** were carried out on a high-vacuum line, with the temperature being increased gradually to 140 °C. Since **2** loses btmse at 70−80 °C to give **1**, both experiments gave the same product of thermolysis. At the final temperature a blue waxy solid condensed on the walls cooled to room temperature. The blue solid crystallized when kept for a longer time at room temperature. The nonvolatile residue was negligible, and the gas evolved from **1** was hydrogen. The blue product was resublimed in the same way to ascertain that no **1** was transferred under high-vacuum conditions. The product was crystallized from a minimum quantity of hexane to give blue crystals. Evaporation of the mother liquor afforded the same blue product without indication of any impurity. The crystals were suitable for X-ray diffraction analysis, which revealed that the structure of the product is that of the double tucked-in derivative of **1**, [Ti{η^3:η^4-C$_5$Me$_2$(SiMe$_3$)(CH$_2$)$_2$}{η^5-C$_5$Me$_4$(SiMe$_3$)}] (**3**). The ^{1}H, ^{13}C, and ^{29}Si NMR spectra of **3** were fully assigned using 1D NOESY, gCOSY, and APT, proving that the double tucked-in ligand is asymmetric. The exo methylene groups are nonequivalent; the group close to the silyl group shows doublets at δ_H 1.03 and 1.14 ppm. However, the distant group gives only a singlet at δ_H 1.11 ppm. The singlet resonance for one of the exo methylene groups was previously observed in the double tucked-in complex [Ti{η^3:η^4-C$_5$Me$_2$R(CH$_2$)$_2$}{η^5-C$_5$Me$_4$R)}] for R = 4-fluorophenyl,[8a] whereas for R = H,[4b] Ph, CH$_2$Ph,[8a] and *ansa*-{O(SiMe$_2$)$_2$}$_{1/2}$[8b] both doublets were observed. A very small separation of doublets for R = CH$_2$Ph (0.01 ppm)[8a] shows that the resonances can be close to degenerate and, hence, cannot be resolved. In undecoupled ^{13}C spectra the exo methylene groups at δ_C 70.38 and 71.88 ppm give J_{CH} = 151.7 and 150.6

(5) (a) Hitchcock, P. B.; Kerton, F. M.; Lawless, G. A. *J. Am. Chem. Soc.* **1998**, *120*, 10264−10265. (b) Horáček, M.; Kupfer, V.; Thewalt, U.; Štěpnička, P.; Polášek, M.; Mach, K. *Organometallics* **1999**, *18*, 3572−3578. (c) Lukešová, L.; Horáček, M.; Štěpnička, P.; Fejfarová, K.; Gyepes, R.; Císařová, I., Kubišta, J.; Mach, K. *J. Organomet. Chem.* **2002**, *659*, 186−196. (d) Lukešová, L.; Pinkas, J.; Horáček, M.; Gyepes, R.; Kubišta, J.; Mach, K. *J. Organomet. Chem.* **2006**, *691*, 748−758.

(6) Reviews on titanocene−btmse complexes: (a) Rosenthal, U.; Burlakov, V. V.; Arndt, P.; Baumann, W.; Spannenberg, A. *Organometallics* **2003**, *22*, 884−900. (b) Rosenthal, U.; Burlakov, V. V. In *Titanium and Zirconium in Organic Synthesis*; Marek, I., Ed.; Wiley-VCH: Weinheim, Germany, 2002; p 355. (c) Rosenthal, U.; Pellny, P.-M.; Kirchbauer, F. G.; Burlakov, V. V. *Acc. Chem. Res.* **2000**, *33*, 119−129.

(7) Horáček, M.; Hiller, J.; Thewalt, U.; Polášek, M.; Mach, K. *Organometallics* **1997**, *16*, 4185−4191.

(8) (a) Kupfer, V.; Thewalt, U.; Tišlerová, I.; Štěpnička, P.; Gyepes, R.; Kubišta, J.; Horáček, M.; Mach, K. *J. Organomet. Chem.* **2001**, *620*, 39−50. (b) Horáček, M.; Štěpnička, P.; Kubišta, J.; Gyepes, R.; Císařová, I.; Petrusová, L.; Mach, K. *J. Organomet. Chem.* **2002**, *658*, 235−241. (c) Horáček, M.; Štěpnička, P.; Gyepes, R.; Císařová, I.; Polášek, M.; Mach, K.; Pellny, P.-M.; Burlakov, V. V.; Baumann, W.; Spannenberg, A.; Rosenthal, U. *J. Am. Chem. Soc.* **1999**, *121*, 10638−10639.

Hz, the coupling constants pertinent to sp^2 hybridization. In agreement with other double tucked-in titanocene compounds[3,4b,8] the mass spectrum of **3** shows the molecular ion as a base peak. The infrared spectrum contains a weak absorption band at 3050 cm^{-1} due to two exo methylene groups, and the electronic absorption spectrum a distinct band at 585 nm. The latter band is close to the absorption band of V (590 nm),[4b] which indicates that the impact of the trimethylsilyl group on the electronic structure of the double tucked-in derivative is negligible.

The thermolytic evolution of hydrogen from titanocene **1** as described in eq 1 is likely a general thermolytic pathway for silyl-containing titanocenes.

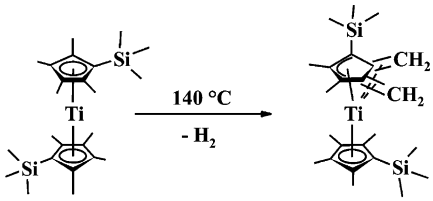

1 **3** (1)

The recently reported isopropyldimethylsilyl group containing titanocene [Ti{η^5-C_5Me_4($SiMe_2$-*i*-Pr)}$_2$] (**1A**)[5d] also afforded the double tucked-in complex [Ti{η^3:η^4-C_5Me_2($SiMe_2$-*i*-Pr)(CH_2)$_2$}-{η^5-C_5Me_4($SiMe_2$-*i*-Pr)}] (**3A**) by vacuum sublimation. Its waxy solid appearance prevented its solid structure determination. However, its NMR spectra showed all features known from the spectra of **3**, proving its purity. The identity of **3A** was further corroborated by its blue color (λ_{max} 580 nm) and ν(C−H) band of low intensity at 3050 cm^{-1}, similarly to **3**.

The thermolysis of **1** in solution in a closed system is less suitable because the hydrogen evolved increases the inner pressure (*danger of explosion*) and can hinder the completion of the thermolysis to **3**. After a toluene solution of **1** was heated in a sealed ampule with an attached UV cell to 140 °C for 8 h, compound **1** was still present in the solution in addition to **3** and hydrogen. In these experiments titanocene **1** proved to be stable at 90 °C for 18 h. Its marginal thermolysis was indicated by a trace of liberated hydrogen after heating to 100 °C for 14 h.

For investigation of the thermolytic behavior of the Ti−methyl derivatives of **1**, the titanocene monomethyl complex [TiMe(η^5-C_5Me_4($SiMe_3$)$_2$] (**5**) and titanocene dimethyl complex [$TiMe_2${η^5-C_5Me_4($SiMe_3$)}$_2$] (**6**) were prepared by methylation of [TiCl(η^5-C_5Me_4($SiMe_3$)$_2$] and [$TiCl_2${η^5-C_5Me_4($SiMe_3$)}$_2$],[9] respectively, with an excess of solid LiMe suspension in hexane. Both compounds were analytically characterized, and the X-ray crystal structure of **5** was determined (see below). In contrast to exclusive activation of cyclopentadienyl methyl groups of **1**, the thermolysis of **5** in toluene at only 90 °C cleanly yielded the known compound **4**. Compounds **4** and **5** are paramagnetic Ti(III) complexes having virtually identical ligand coordination, and hence, they do not differ significantly in their ESR and electronic absorption spectra. They were easily distinguished by their EI-MS spectra, since **5** showed only a low abundant molecular ion (*m*/*z* 449) and *m*/*z* 434 [M − Me]$^+$ as a base peak, whereas the base peak of **4** is the molecular ion (*m*/*z* 433). The identity of the thermolytic product with the published structure of **4**[7] was confirmed by X-ray diffraction analysis of its single crystal. The present result affords clear evidence that the methyl radical generated in the homolysis of the Ti−Me bond abstracts a hydrogen atom selectively from the trimethylsilyl group (eq 2).

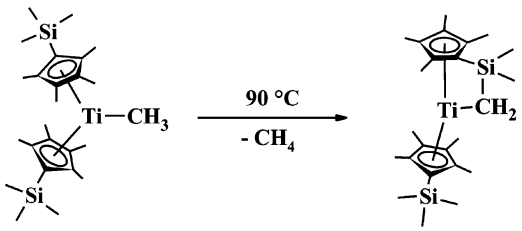

5 **4** (2)

The thermolysis of **6** in toluene solution was indicated by the change of its orange-yellow color to green. It occurred at 90 °C and was complete within 12 h. At higher temperatures the thermolysis required a shorter time, affording the same product in practically quantitative yield. The structure of this product was deduced from its NMR spectra and confirmed by X-ray diffraction analysis to be [Ti{η^6:η^1-C_5Me_3(CH_2)($SiMe_2$-CH_2)}{η^5-C_5Me_4($SiMe_3$)}] (**7**). Methane was the only detected gaseous product (eq 3). The presence of one metal tucked-in

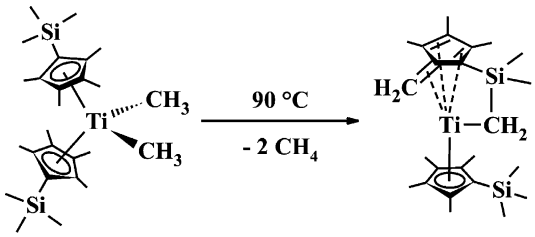

6 **7** (3)

exo methylene group and one σ-Ti−CH_2Si grouping on the same cyclopentadienyl ring was cleanly observed in ^{1}H and ^{13}C NMR spectra. The ^{1}H NMR spectrum exhibited seven signals for the methyl groups of the cyclopentadienyl rings, two singlets for diastereotopic methyls of the $SiMe_2$ group, and one signal for the $SiMe_3$ group in the expected intensity ratios. The doublets diagnostic for TiCH_2Si were observed at −3.95 and −0.57 ppm with $^2J_{HH}$ = 12.9 Hz, in agreement with similar high-field resonances for ZrCH_2Si and TiCH_2Si moieties.[10] In ^{13}C NMR spectra, the TiCH_2Si signal appeared at 37.48 ppm (dd, $^1J_{CH}$ = 114.0 Hz, $^1J_{CH}$ = 132.6 Hz). Nondecoupled gHSQC allowed us to assign the lower value of $^1J_{CH}$ to the splitting by the high-field proton (−3.95 ppm). Both of these features classify this C−H bond as exerting a strong agostic interaction with the metal. Signals of diastereotopic protons of the exo methylene group are overlapped by stronger methyl signals; their chemical shifts at 1.15 and 2.06 ppm were determined from cross-peaks in the gCOSY spectrum. The ^{1}D NOESY experiment with irradiation of the vicinal methyl group C(3) showed a close through-space contact with the proton at δ 2.06 ppm. The =CH_2 signal was found at 77.14 ppm (t, $^1J_{CH}$ = 150.6 Hz), the values typical of the double tucked-in titanocene compounds.[8] The presence of one η^5-C_5Me_4($SiMe_3$) ligand was proved by gHMBC, where indicative cross-peaks allow assignment of two methyl signals at 1.64 and 2.17 ppm in proximal and two methyl

(9) Horáček, M.; Gyepes, R.; Císařová, I.; Polášek, M.; Varga, V.; Mach, K. *Collect. Czech. Chem. Commun.* **1996**, *61*, 1307−1320.

(10) Zr: (a) Horáček, M.; Štěpnička, P.; Kubišta, J.; Fejfarová, K.; Gyepes, R.; Mach, K. *Organometallics* **2003**, *22*, 861−869. (b) Choukroun, R.; Wolff, F.; Lorber, C.; Donnadieu, B. *Organometallics* **2003**, *22*, 2245−2248. (c) Pool, J. A.; Lobkovsky, E.; Chirik, P. J. *J. Am. Chem. Soc.* **2003**, *125*, 2241−2251. (d) Bernskoetter, W. H.; Pool, J. A.; Lobkovsky, E.; Chirik, P. J. *Organometallics* **2006**, *25*, 1092−1100. Ti: (d) Hanna, T. E.; Keresztes, I.; Lobkovsky, E.; Bernskoetter, W. H.; Chirik, P. J. *Organometallics* **2004**, *23*, 3448−3458.

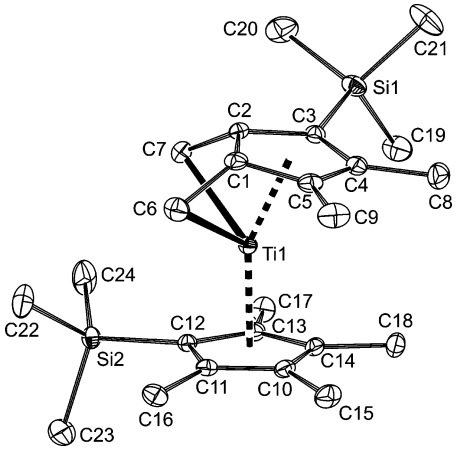

Figure 1. PLATON drawing of **3** with 30% probability thermal ellipsoids and the atom-numbering scheme. For clarity, all hydrogen atoms are omitted.

signals at 1.30 and 1.76 ppm in distant position to the trimethylsilyl group. Compound **7** displayed EI-MS spectra consisting of the molecular ion as a base peak and a few low-abundant fragment ions. The exo methylene infrared absorption band occurred at 3062 cm^{-1} and was very weak. The electronic absorption spectrum of **7** displayed an absorption band at 624 nm, compatible with the ligand coordination in a fulvene manner, as in **IV**.[1b−d] The X-ray diffraction analysis of **7**, although affording data of poor quality, confirmed the structure outlined above. An attempt to optimize the molecular parameters obtained from diffraction data by DFT calculations led to negligible changes only. These calculations also indicated an agostic nature of the silylmethylene protons, the exo proton (δ −3.75 ppm) showing much stronger agostic interaction with titanium (see below).

The mechanism of the formation of **7** is unknown, since no intermediate of the thermolysis of **6** was captured at the lowest thermolytic temperature. Since the leaving methyl group from the dissociating Ti−Me bond in **5** abstracts exclusively one hydrogen atom from the trimethylsilyl group to give **4**, a similar step is expected to initiate the thermolysis of **6**. This step is to be rapidly followed by the hydrogen abstraction from the cyclopentadienyl methyl group adjacent to the silyl substituent to give **7**. Such a step proceeds very slowly in the thermolysis of **1** to **3** at 100 °C; however, a suggested silylmethylene intermediate with an easily dissociating methyl group and inclined cyclopentadienyl ring can allow for its rapid course at 90 °C. On the other hand, the formation of **3** from **1** probably does not involve the intermediate hydrogen abstraction from the trimethylsilyl group, because conversion of **7** to **3** has not been observed at 140 °C.

Crystal Structure of 3. The asymmetric molecule of **3** (Figure 1) has a common structure of double tucked-in titanocene complexes bearing four methyl groups and a different substituent on each cyclopentadienyl ligand: i.e., two vicinal exo methylene groups in the neighborhood of the substituent on only one ligand. The only exception is the benzyl substituent, which converts into the exo benzylidene group.[8a] The quantitative geometric parameters of the allyldiene moiety (Table 1) differ only slightly from those found for the allyldiene compounds with the benzyl, phenyl,[8a] and *ansa*-$O(SiMe_2)_2$ substituents[8b] or H.[8c] For a detailed discussion of the structure of **3**, see the Supporting Information.

Crystal Structure of 5. Essential molecular geometric parameters are given in Table 2, and the PLATON drawing of

Table 1. Selected Bond Lengths (Å) and Bond Angles (deg) for 3

Ti−Cg(1)[a]	1.9487(8)	Ti−Cg(2)[a]	2.0315(8)
Ti-Cg(3)[b]	1.7534(10)	Ti−C(1)	2.0886(17)
Ti−C(2)	2.0826(17)	Ti−C(3)	2.3890(17)
Ti−C(4)	2.5390(17)	Ti−C(5)	2.3680(17)
Ti−C(6)	2.272(2)	Ti−C(7)	2.245(2)
C(1)−C(6)	1.433(3)	C(2)−C(7)	1.434(3)
C(1)−C(2)	1.459(2)	C(2)−C(3)	1.456(2)
C(3)−C(4)	1.423(2)	C(4)−C(5)	1.405(3)
C(1)−C(5)	1.443(3)	C−C(10−14)	1.418−1.435(3)
C(3)−Si(1)	1.8770(18)	C(12)−Si(2)	1.8760(17)
$Si-C(Me)_{av}$	1.866(2)		

Cg(1)−Ti−Cg(2)	154.64(3)	C(6)-Ti−C(7)	76.83(8)
Ti−C(6)−C(1)	64.02(10)	Ti−C(7)−C(2)	64.62(10)
C(1)−C(2)−C(3)	107.66(15)	C(2)−C(1)−C(5)	106.82(15)
C(2)−C(3)−C(4)	106.89(15)	C(1)−C(5)−C(4)	108.53(15)
C(3)−C(4)−C(5)	110.09(16)	C(11)−C(12)−C(13)	106.32(14)
$C-C-C(Cp)_{av}$[c]	108.41(15)	C(2)−C(3)−Si(1)	125.89(13)
C(4)−C(3)−Si(1)	125.68(13)	C(11)−C(12)−Si(2)	125.26(13)
C(13)−C(12)−Si(2)	128.08(13)	φ[d]	10.40(12)
ψ[e]	42.46(10)		

[a] Cg(1) and Cg(2) are centroids of the C(1−5) and C(10−14) cyclopentadienyl rings, respectively. [b] Cg(3) is a centroid of the tetragon determined by the C(1), C(2), C(6), and C(7) atoms. [c] Angles within the cyclopentadienyl ring C(10−14). except C(11)−C(12)−C(13). [d] Dihedral angle between the least-squares cyclopentadienyl ring planes. [e] Dihedral angle between the least-squares planes of C(1−5) and C(1), C(2), C(6), and C(7).

Table 2. Selected Bond Lengths (Å) and Bond Angles (deg) for 5

Ti−Cg(1)[a]	2.0808(4)	Ti−C(25)	2.213(2)
Ti−Cg(2)	2.0791(4)	Si(1)−C(1)	1.8707(16)
Ti−C(Cp)	2.3750(15)−2.4270(16)	Si(2)−C(13)	1.8712(16)
C−C(Cp)	1.412(2)−1.442(2)	Si−C(Me)	1.865(2)−1.870(2)

Cg(1)−Ti−Cg(2)	145.94(2)	C(2)−C(1)−Si(1)	123.06(11)
Cg(1)−Ti−C(25)	106.91(7)	C(5)−C(1)−Si(1)	130.43(11)
Cg(2)−Ti−C(25)	107.15(7)	C(14)−C(13)−Si(2)	130.61(11)
C(2)−C(1)−C(5)	105.57(11)	C(17)−C(13)−Si(2)	122.58(11)
C(14)−C(13)−C(17)	105.79(12)	φ[c]	34.51(6)
$C-C-C(Cp)_{av}$[b]	108.56(13)		

[a] Cg(1) and Cg(2) are centroids of the C(1−5) and C(13−17) cyclopentadienyl rings, respectively. [b] Angles within the cyclopentadienyl rings, except those at C(1) or C(13). [c] Dihedral angle between the least-squares cyclopentadienyl planes.

5 is shown in Figure 2. The structure of **5** shows the pseudo-trigonal coordination around the titanium atom common for persubstituted titanocene monochlorides having the η^5-C_5Me_4-*t*-Bu,[11] η^5-C_5Me_4Ph,[12] and η^5-$C_5Me_4SiMe_3$ ancillary ligands.[9] The bulky substituents occupy positions on opposite sides of the plane defined by Cg(1), Ti, and Cg(2) so that the steric hindrance in hinge positions of staggered cyclopentadienyl ligands is similar to that in the permethylated [$TiCl(\eta^5$-$C_5Me_5)_2$].[13] The only known crystal structure of a titanocene carbyl compound comparable to **5** is that of [$Ti(CH_2CMe_3)(\eta^5$-$C_5Me_5)_2$]; however, the bent neopentyl group introduces a steric congestion into the open shell side of the titanocene skeleton.[14] As a result, its Cg(1)−Ti−Cg(2) angle of 139.4(3)° is smaller than in **5** (145.94(2)°). The magnitude of the latter angle is comparable with that found for [$TiF(\eta^5$-$C_5Me_5)_2$] (ca. 145°)[15]

(11) Lukešová, L.; Gyepes, R.; Horáček, M.; Kubišta, J.; Čejka, J.; Mach, K. *Collect. Czech. Chem. Commun.* **2005**, *70*, 1589−1603.
(12) Horáček, M.; Polášek, M.; Kupfer, V.; Thewalt, U.; Mach, K. *Collect. Czech. Chem. Commun.* **1999**, *64*, 61−72.
(13) Pattiasinna, J. W.; Heeres, H. J.; van Bolhuis, F.; Meetsma, A.; Teuben, J. H. *Organometallics* **1987**, *6*, 1004−1010.
(14) Luinstra, G. A.; ten Cate, L. C.; Pattiasinna, J. W.; Meetsma, A.; Teuben, J. H. *Organometallics* **1991**, *10*, 3227−3237.
(15) Lukens, W. W.; Smith, M. R., III; Andersen, R. A. *J. Am. Chem. Soc.* **1996**, *118*, 1719−1728.

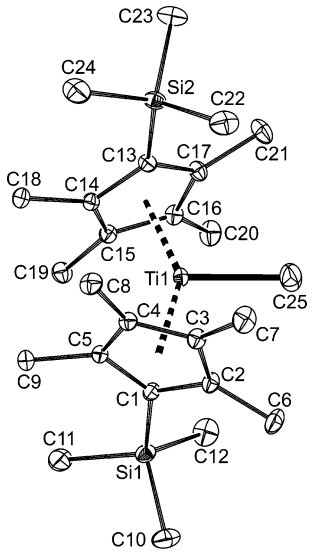

Figure 2. PLATON drawing of **5** with 30% probability thermal ellipsoids and the atom-numbering scheme. For clarity, all hydrogen atoms are omitted.

and larger than for [Ti(NH_2)(η^5-C_5Me_5)$_2$] (ca. 144.3°),[16] [TiCl-(η^5-C_5Me_5)$_2$] (143.6(2)°),[13] or [Ti(OH)(η^5-C_5Me_5)$_2$] (143.79-(5)°),[17] which means that the methyl substituent causes a surprisingly low steric hindrance toward the cyclopentadienyl ligands.[18] A large Cg−Ti−Cg angle similar to that in **5** was also found in the acetylides [Ti(C≡$CCMe_3$)(η^5-C_5Me_5)$_2$][19a] and [Ti(C≡$CCMe_3$)(η^5-C_5Me_4Ph)$_2$].[19b]

Crystal Structure of 7. The geometric parameters of **7** were obtained with low precision; however, they were reliable enough to establish the atom connectivity and essential molecular features. The important bond lengths and angles are given in Table 3 and the molecular structure with atom labeling is shown in Figure 3. Both cyclopentadienyl rings are planar (deviations from the least-squares planes $<\pm0.02(1)$Å), and their Ti−Cg distances are virtually equal. The ring C(1−5) is, however, remarkably tilted, showing the shortest Ti−C(2) bond length of 2.172(14) Å and the longest Ti−C(4) bond length of 2.637-(15) Å. The tucked-in methylene Ti−C(6) bond length of 2.249-(14) Å falls into the range of the bond lengths found for double tucked-in titanocene complexes,[8] including **3**, and for the single tucked-in titanocene [Ti^{III}\{η^5:η^1-$C_5Me_4(CH_2)$\}(η^5-C_5Me_5)][20a] or its complex with $B(C_6F_5)_3$, [Ti^{IV}\{η^5:η^1-$C_5Me_3(CH_2)CH_2B(C_6F_5)_3$\}($\eta^5$-$C_5Me_5$)].[20b] The angle between the cyclopentadienyl least-squares planes φ (27.6(6)°) is much larger than that in **3** (10.4(1)° and slightly smaller than that in **4** (30.2°).[7] The strain due to the bridging Ti−C bonds causes deviations of the C(6) and Si(1) atoms from the cyclopentadienyl least-squares plane as much as 0.88(2) and 0.63(2) Å toward the titanium atom, respectively. All of the other methyl carbon atoms and Si(2) are declined in opposite direction (maximum 0.27(2) Å for C(18)).

Table 3. Selected Bond Lengths (Å) and Bond Angles (deg) for 7

Ti−Cg(1)[a]	2.078(8)	Ti−Cg(2)	2.074(7)
Ti−C(1)	2.295(15)	Ti−C(2)	2.172(14)
Ti−C(3)	2.423(14)	Ti−C(4)	2.637(15)
Ti−C(5)	2.521(16)	Ti−C(6)	2.249(14)
Ti−C(10)	2.201(15)	C(2)−C(6)	1.43(2)
Si(1)−C(1)	1.831(16)	Si(1)−C(10)	1.841(15)
Ti−C(13−17)	2.368−2.425(14)	Si(2)−C(13)	1.878(14)

Cg(1)−Ti−Cg(2)	144.4(3)	C(2)−Ti−C(6)	37.7(5)
C(6)−C(2)−Ti	74.0(8)	C(6)−Ti−C(10)	91.2(6)
Ti−C(10)−Si(1)	97.6(6)	C(1)−Si(1)−C(10)	93.7(7)
C(2)−C(1)−C(5)	103.2(13)	C(14)−C(13)−C(17)	104.9(12)
C(13)−Si(2)−C(Me)$_{av}$	111.0(7)	C(1)−Si(1)−C(10)	93.7(7)
C−C−C(Cp)[b]$_{av}$	109.2(13)	C−C−C(Cp)[c]$_{av}$	108.8(11)
C(2)−C(1)−Si(1)	122.6(11)	C(5)−C(1)−Si(1)	127.5(11)
C(14)−C(13)−Si(2)	122.6(10)	C(17)−C(13)−Si(2)	132.0(11)
φ[d]	27.63(67)		

[a] Cg(1) and Cg(2) are centroids of the C(1−5) and C(10−14) cyclopentadienyl rings, respectively. [b] Angles in the cyclopentadienyl ring C(1−5), except C(2)−C(1)-C(5). [c] Angles in the cyclopentadienyl ring C(13−17), except C(14)−C(13)-C(17). [d] Dihedral angle between the least-squares cyclopentadienyl ring planes.

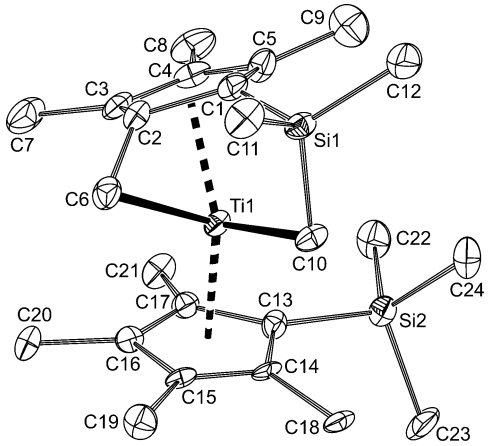

Figure 3. PLATON drawing of **7** with 30% probability thermal ellipsoids and the atom-numbering scheme. For clarity, all hydrogen atoms are omitted.

Reasons for the Thermal Stability of Titanocene 1. The low thermal stability of titanocenes has been generally attributed to the low number of metal valence electrons (14 ve), while the paramagnetism of titanocenes is due to the presence of two d electrons.[1a,b,5] As was anticipated earlier,[21] only two of the five d orbitals (d_{xz}, d_{yz}) should be involved in the bonding interaction with the cyclopentadienyl carbon p orbitals, and the remaining three d orbitals should accommodate the two electrons, giving a triplet state molecule. Our DFT calculations for **1** determined the energies of frontier orbitals and confirmed the involvement of the metal d orbitals in them, in general agreement with DFT studies for other metallocenes.[22] The actual metal−ligand interaction was revealed to be mediated through two disparate three-center−four-electron (3c4e) bonds. Both the cyclopentadienyl ligands and the titanium atom act as three distinct centers, which generate one pair of fully bonding (Figure 4) and one pair of complementary antibonding orbitals (Figure 5). Orienting the *z* axis of the coordinate system through the cyclopentadienyl centroids, these interactions utilize the d_{xz} and d_{yz} orbitals on the metal. In addition, a further MO pair between the same three centers was also found and classified as the

(16) Brady, E.; Telford, J. R.; Mitchell, G.; Lukens, W. *Acta Crystallogr.* **1995**, *C51*, 558−560.

(17) Horáček, M.; Gyepes, R.; Kubišta, J.; Mach, K. *Inorg. Chem. Commun.* **2004**, *7*, 155−159.

(18) The Cg(1)−Ti−Cg(2) angle is yet larger in [TiH(η^5-C_5Me_5)$_2$] (ca. 152.1°): Lukens, W. W.; Matsunaga, P. T.; Andersen, R. A. *Organometallics* **1998**, *17*, 5240−5247.

(19) (a) Kirchbauer, F. G.; Pellny, P.-M.; Sun, H.; Burlakov, V. V.; Arndt, P.; Baumann, W.; Spannenberg, A.; Rosenthal, U. *Organometallics* **2001**, *20*, 5289−5296. (b) Mach, K.; Gyepes, R.; Horáček, M.; Petrusová, L.; Kubišta, J. *Collect. Czech. Chem. Commun.* **2003**, *68*, 1877−1896.

(20) (a) Fischer, J. M.; Piers, W. E.; Young, V. G., Jr. *Organometallics* **1996**, *15*, 2410−2412. (b) Varga, V.; Šindelá, P.; Císařová, I.; Horáček, M.; Kubišta, J.; Mach, K. *Inorg. Chem. Commun.* **2005**, *8*, 222−226.

(21) Lauher, J. W.; Hoffmann, R. *J. Am. Chem. Soc.* **1976**, *98*, 1729−1742.

(22) Green, J. C. *Chem. Soc. Rev.* **1998**, 263−271.

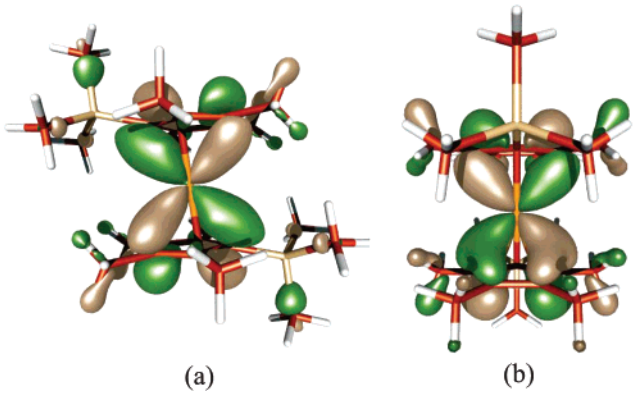

Figure 4. Bonding orbitals (a) 114 ($\epsilon_\alpha = -0.201\ 53$ au) and (b) 115 ($\epsilon_\alpha = -0.201\ 20$ au) for **1**.

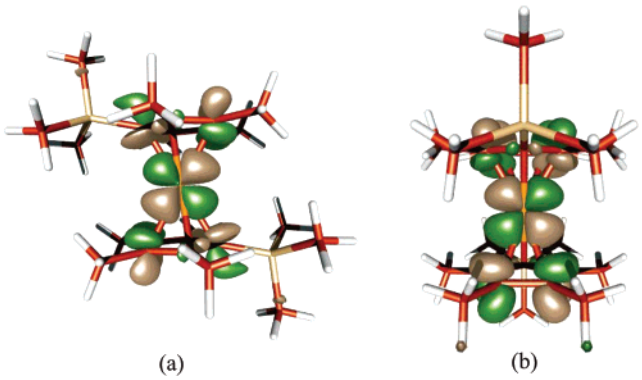

Figure 5. Antibonding orbitals (a) 123 ($\epsilon_\alpha = -0.006\ 53$ au) and (b) 126 ($\epsilon_\alpha = -0.002\ 17$ au) for **1**.

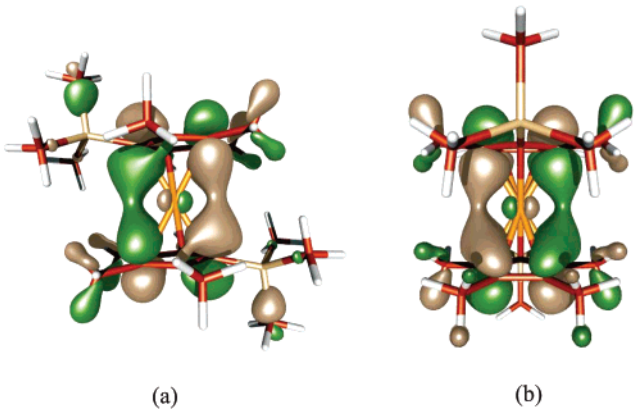

Figure 6. The partially bonding occupied orbitals ((a) 116, $\epsilon_\alpha = -0.187\ 08$ au) and (b) 117 (HOMO), $\epsilon_\alpha = -0.180\ 36$ au) for **1**.

HOMO (Figure 6). They arise from mixing an intramolecular $\pi-\pi$ bonding interaction between the two cyclopentadienyl rings and an antibonding interaction with the metallic center. The contribution of both of these HOMO's to the overall bonding in the titanocene is significant, since their energies (ϵ_a) are surprisingly low. Energies of the three practically nonbonding d orbitals (SOMO d_{xy} and d_{z^2} and LUMO $d_{x^2-y^2}$) are close to each other at an energy about halfway between those for the bonding and the corresponding antibonding MO's.

The type of bonding described above is generally pronounced in highly methyl substituted titanocenes,[23] as already exemplified by a report on thermally stable titanocenes [Ti(η^5-$C_5Me_4R)_2$] (R = *tert*-butyl, isopropyl).[24] An analogous bonding in electron-rich transition-metal metallocenes is unlikely to occur, however, due to strong repulsion by the d orbitals carrying two electrons.[22]

An extraordinary stabilization of **1** is most probably attributable to an additional stabilizing interaction, having its roots in the peculiar properties of the Si−C bond itself. Contrary to expectation, Si−C bonds are by no means similar to C−C σ bonds, since any occupied Si−C bonds happened to be antibonding in all the cases we have studied. The antibonding Si−C interaction transfers the electron density away from the silicon atom, and being sufficiently diffuse, this electron cloud becomes capable of far-ranging interactions with more distant atomic centers. These secondary interactions are able to compensate the energy loss due to the formation of the σ^* bond. We note here that the silicon d orbitals (also included in the calculations) were never found to play any significant role in this stabilizing mechanism.

The stabilization by the $SiMe_3$ group in **1** is demonstrated on the section of MO 113, oriented perpendicularly to the *xy* plane (Figure 7). Assuming C_{2h} symmetry, this section plane contains the Ti atom, both Si atoms, both cyclopentadienyl ipso carbon atoms, and two methyl carbon atoms of both $SiMe_3$ groups. The antibonding interaction between the silicon and its methyl carbon atom results in the formation of an electron cloud, extending even to the titanium center, giving rise to a stabilizing interaction with one of its d orbitals. A table of energies and a graphical representation of all MO orbitals having a significant d character and the interpretation of the electronic absorption spectra of **1** are available in the Supporting Information.

Frontier Molecular Orbitals for 3. The DFT calculation for **3** was carried out to account for its higher thermal stability compared to **1** and to justify the electronic structure, which can be expressed as the σ-methylene structure $Ti^{IV}\{\eta^5$-C_5Me_4-$(SiMe_3)\}\{\eta^5{:}\eta^1{:}\eta^1$-$C_5Me_2(CH_2)_2(SiMe_3)\}$ or the allyldiene structure $Ti^{II}\{\eta^5$-$C_5Me_4(SiMe_3)\}\{\eta^3{:}\eta^4$-$C_5Me_2(CH_2)_2(SiMe_3)\}$.

Using the same coordinate system as for **1**, the unchanged cyclopentadienyl ligand is bonded by a pair of d orbitals, bearing close resemblance to those in **1**. Here, the $\pi-\pi$-like interaction is absent, as the pertinent d orbitals are involved in the bonding of the doubly tucked-in ligand. This is accomplished via two sets of 3c4e bonds, since the four π electrons of the diene system can be accommodated by two MO's, while the allyl system will be present in only one. The fully bonding orbitals for both sets are shown in Figure 8 and their partially bonding/antibonding counterparts in Figure 9. This bonding mechanism utilizes four of the five d orbitals, since both $d_{x^2-y^2}$ and d_{z^2} now participate in the 3c system. The fifth d orbital (d_{xy}) has no appropriate partner(s) to interact with and is the LUMO. The above results thus confirm the correctness of the allyldiene model for the double tucked-in ligand.

The validity of the calculations was verified utilizing the ground-state determinant as the reference for the calculation of the lowest-lying electronic transitions. The results obtained fit the experimental electronic absorption spectrum very well. Orbital energies and details of UV−vis spectra calculations by means of time-dependent DFT are given in the Supporting Information.

Frontier Molecular Orbitals for 7. Unlike the case for **1** and **3**, where the d orbitals did not undergo any significant mixing, thus allowing an easy assignment of their character in individual MO's, the present molecule implements a different orientation of the coordinate system and a rather complicated mixing of the metallic orbitals. In spite of this, it is easily

(23) Gyepes, R. Unpublished DFT calculations on titanocenes.

(24) Hanna, T. E.; Lobkovsky, E.; Chirik, P. J. *J. Am. Chem. Soc.* **2004**, *126*, 14688−14689.

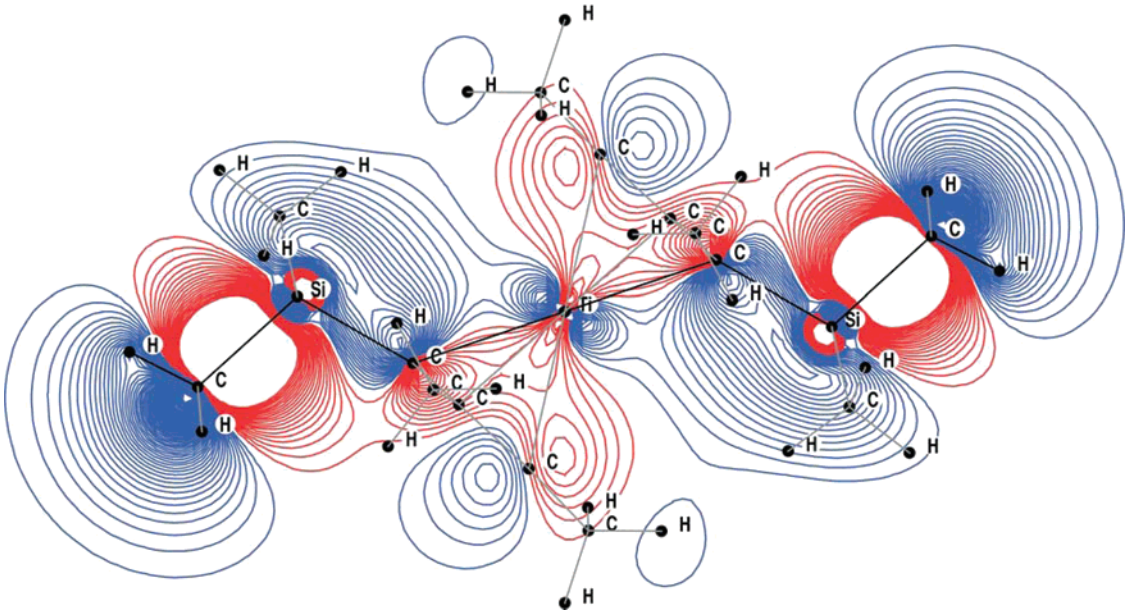

Figure 7. Section of MO 113 ($\epsilon_\alpha = -0.255\ 12$ au) for **1**.

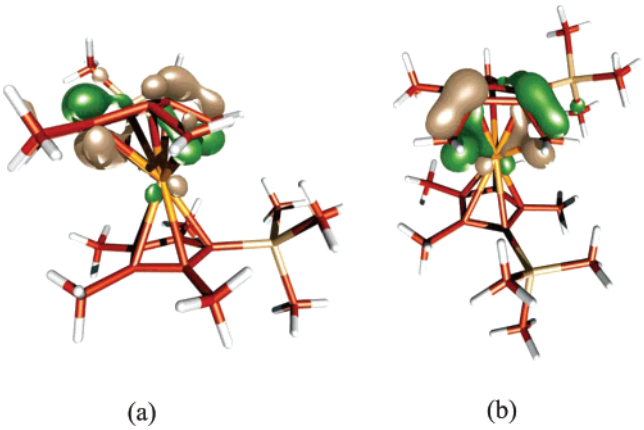

Figure 8. The fully bonding orbitals of the 3c4e bonds ((a) 107, $\epsilon = -0.271\ 15$ au; (b) 108, $\epsilon = -0.268\ 65$ au) for **3**.

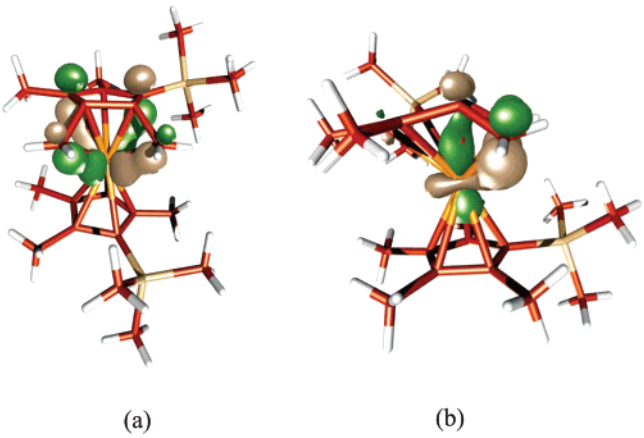

Figure 9. The partially bonding orbitals of the 3c4e bonds ((a) 111, $\epsilon = -0.205\ 96$ au; (b) 112 (HOMO), $\epsilon = -0.182\ 58$ au) for **3**.

recognized that the unchanged cyclopentadienyl ligand is bonded analogously as in **3**, and the silylmethylene group is σ bonded to the metal. The exo methylene group is bonded via one set of three-center MO's (Figures 10 and 11). Although **7** utilizes four of its five titanium d orbitals and should be thus fairly stable already on its own, its stability is further enhanced by a long-range interaction between the metal and one Si−C σ* bond. In addition to the regular Ti−C σ bond, the metallic center benefits from an auxiliary stabilizing interaction with the Si−C σ* bond (Figure 12).

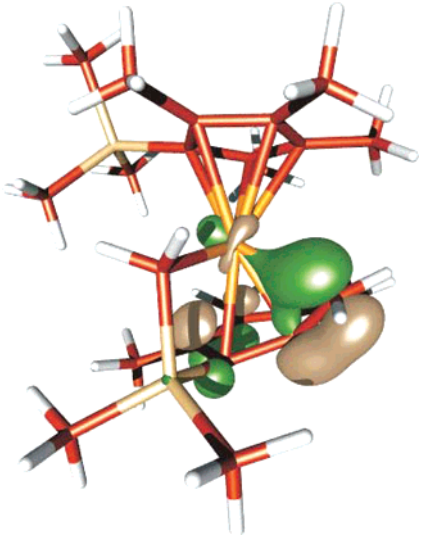

Figure 10. The fully bonding three-center orbital 107 ($\epsilon = -0.267\ 90$ au) in **7**.

On the basis of the MO's obtained from DFT studies, the agostic interaction of the two hydrogen atoms in the Si−CH_2 moiety (vide supra) could also be examined. Due to the suboptimal quality of the solid-state structure, however, prior to further theoretical studies, a geometry optimization was carried out. The optimized structure had both C−H bonds lengthened to 1.09 Å, while the Ti−C−H angles became 111.13° for the hydrogen atom closer to the exo methylene group and 108.42° for the other. From geometrical requirements for agostic bonding[25] it follows that a smaller Ti−C−H angle relates to a stronger agostic interaction. According to GIAO

(25) (a) Brookhart, M.; Green, M. L. H. *J. Organomet. Chem.* **1983**, *250*, 395−408. (b) Braga, D.; Grepioni, F.; Tedesco, E.; Biradha, K.; Desiraju, G. R. *Organometallics* **1997**, *16*, 1846−1856. (c) Thakur, T. S.; Desiraju, G. R. *Chem. Commun.* **2006**, 552−555. (d) Raos, N.; Pavlovic, G. *Kem. Ind.* **2006**, *55*, 167−174.

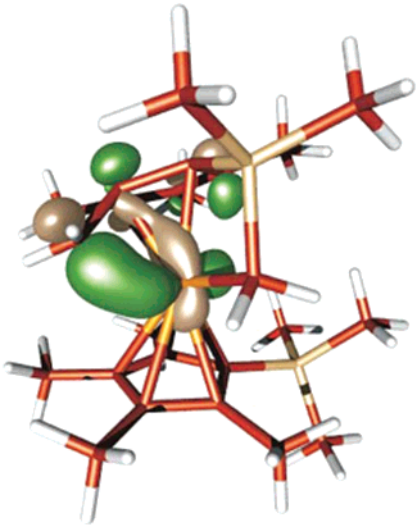

Figure 11. The partially bonding three-center HOMO orbital 112 ($\epsilon = -0.190\ 96$ au) in **7**.

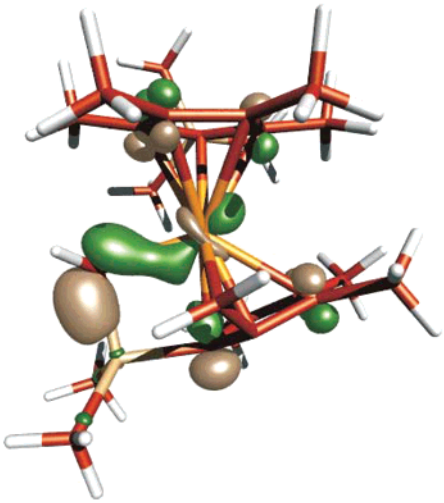

Figure 12. Orbital 111 ($\epsilon = -0.208\ 54$ au) in **7**, showing the stabilizing interaction of the Si−CH_2 group with the metal.

results for the optimized structure, the chemical shifts of the two hydrogen atoms were separated by 2.5 ppm, in reasonable agreement with the experimental value of 3.4 ppm.

The nonequivalence of the two hydrogen atoms arises from the interaction of their C−H bonds with the two occupied 3c orbitals of different energy. The C−H bond involving the hydrogen atom with a smaller upfield shift donates to the HOMO 112 (Figure 11), while the other donates to the fully bonding 3c MO 107 (Figure 10). Since the HOMO is of partially antibonding nature, its energy is more distant from that of the C−H bond, allowing for a weaker agostic interaction than for the other C−H bond. Orbitals 112 and 107 at the 3% and 2% probability levels, respectively, showing the agostic interactions, the table of relevant orbital energies, and their graphical representations are given in the Supporting Information.

Conclusions

Thermolytic experiments with **1**, **5**, and **6** summarized in Scheme 2 showed that titanocene **1** was thermally more stable than its Ti−methyl derivatives and the respective thermolytic products **3**, **4**, and **7** were stable, at least at 140 °C. In comparison with the thermal stabilities of permethyltitanocene

Scheme 2

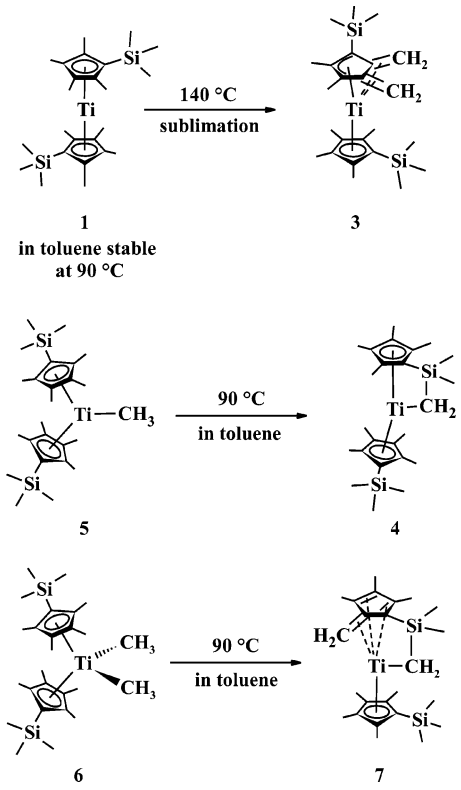

I and its mono- and dimethyl Ti derivatives (Scheme 1), the trimethylsilyl substituent increased the thermal stability of **1** and destabilized **5** and **6**. Reasons for the high thermal stability of **1**, **3**, and **7** have been tentatively rationalized by DFT calculations. For **1** they showed that Si−C bonds can generate distant electron density capable of interacting with "nonbonding" metal d orbitals in a bonding manner. The other additional bonding $\pi-\pi$ interactions between the cyclopentadienyl rings seem to be common for electron-poor titanocene moieties with parallel cyclopentadienyl rings.[23] For the thermolysis of **5** and **6** it can be anticipated that a diffuse electron density which is generated from the Si−C bonds and extends to the proximity of the titanium atom facilitates the dissociation of the Ti−Me bond(s) followed by a hydrogen abstraction specifically from the trimethylsilyl group. A higher thermal stability of **3** and **7** compared to that of **1** is due to exploitation of four against two titanium d orbitals for bonding. The exomethylene groups in the tucked-in compounds **3** and **7** are bonded via 3c bonds. The shapes of relevant orbitals are compatible with the assignment of activated ligands to $\eta^3{:}\eta^4$-allyldiene and $\eta^6{:}\eta^1$-fulvene structures, respectively, although the ligand π systems are not planar as required for the canonical structure. The alternative ligand bonding using σ-Ti−C bonds, i.e., $\eta^5{:}\eta^1{:}\eta^1$, can be considered as a minor canonical structure admixture. The NMR behavior of the exo methylene groups, IR bands near 3050 cm^{-1}, and electronic absorption bands close to 600 nm exclude this type of bonding as a major one.

Experimental Section

General Considerations. Synthesis of the silylated titanocene dichloride $[TiCl_2\{\eta^5\text{-}C_5Me_4(SiMe_3)\}_2]$ was carried out under an argon atmosphere.[9] Further reactions with this compound, leading to σ- or π-organyl titanium derivatives, were performed under vacuum of a vacuum line in sealed all-glass devices equipped with breakable seals. ^1H (300 MHz), ^{13}C (75 MHz), and ^{29}Si (59.6 MHz)

NMR spectra were recorded on a Varian Mercury 300 spectrometer in C_6D_6 solutions at 25 °C. Chemical shifts (δ/ppm) are given relative to the residual solvent signal (δ_H 7.15) and to the solvent resonance (δ_C 128.00). The δ_{Si} values are referenced to tetramethylsilane. The standard NMR techniques as APT, 1D NOESY, gCOSY, gHSQC, and gHMBC were used for detailed assignments of the signals. EI-MS spectra were obtained on a VG-7070E mass spectrometer at 70 eV. Crystalline samples in sealed capillaries were opened and inserted into the direct inlet under argon. The spectra are represented by the peaks of relative abundance higher than 7% and by important peaks of lower intensity. Crystals for EI-MS measurements and melting point determinations were placed in glass capillaries in a Labmaster 130 glovebox (mBraun) under purified nitrogen (concentrations of oxygen and water were lower than 2.0 ppm) and sealed with a flame. KBr pellets were prepared in the glovebox and placed in an air-protecting cuvette, and IR spectra were measured on a Nicolet Avatar FT IR spectrometer in the range 400−4000 cm^{-1}. ESR spectra were recorded on an ERS-220 spectrometer (Center for Production of Scientific Instruments, Academy of Sciences of the GDR, Berlin, Germany) operated by a CU-1 unit (Magnettech, Berlin, Germany). g values were determined by using an Mn^{2+} standard at $g = 1.9860$ ($M_I = -1/2$ line). An STT-3 variable-temperature unit was used for measurements in the range −196 to +25 °C. UV−near-IR spectra in the range 280−2000 nm were measured on a Varian Cary 17D spectrometer in all-sealed quartz cells (Hellma).

Chemicals. The solvents THF, hexane, and toluene were dried by refluxing over $LiAlH_4$ and stored as solutions of the green dimeric titanocene $[(\mu\text{-}\eta^5{:}\eta^5\text{-}C_5H_4C_5H_4)(\mu\text{-}H)_2\{Ti(\eta^5\text{-}C_5H_5)\}_2]$.[26] C_6D_6 (99.5% D) was degassed, distilled on a vacuum line into a storage ampule containing dimeric titanocene, and stored as its solution. The titanocene dichloride $[TiCl_2\{\eta^5\text{-}C_5Me_4(SiMe_3)\}_2]$ and titanocene chloride $[TiCl\{\eta^5\text{-}C_5Me_4(SiMe_3)\}_2]$ were prepared as described elsewhere.[9] $[TiCl_2(\eta^5\text{-}C_5Me_5)_2]$ and methyllithium (LiMe) in diethyl ether were purchased from Aldrich. The titanocene $[Ti^{II}\{\eta^5\text{-}C_5Me_4(SiMe_3)\}_2]$ (**1**) and its complex with bis(trimethylsilyl)ethyne (btmse), $[Ti(\eta^2\text{-btmse})\{\eta^5\text{-}C_5Me_4(SiMe_3)\}_2]$ (**2**), were synthesized as previously reported.[5b]

Thermolysis of 1 To Give $[Ti\{\eta^5\text{-}C_5Me_4(SiMe_3)\}\{\eta^3{:}\eta^4\text{-}C_5Me_2(SiMe_3)(CH_2)_2\}]$ (3). Titanocene **1** (0.3 g, 0.87 mmol) was dissolved in toluene, and the solution was transferred to a distillation ampule on a vacuum line and evaporated under vacuum with successive heating up to 140 °C. A blue product condensed on a tube wall outside the oven. This was dissolved in toluene, and the solution was used to repeat the distillation to ascertain that no **1** was present in the distillate. The blue distillate, which crystallized after cooling to room temperature, was dissolved in hexane, and the product crystallized from 2.0 mL of the solution by cooling to −28 °C for 2 days. Blue crystals of **3** were separated from the blue mother liquor and dried under vacuum. Yield: 0.34 g (65%). The mother liquor was evaporated under vacuum, leaving a blue solid. Its NMR spectra in C_6D_6 were identical with those of the crystalline product. Hence, the yield of **3** was practically quantitative.

Data for **3** are as follows. Mp 89 °C. EI-MS (80 °C): *m*/*z* (relative abundance) 435 (8), 434 (28), 433 (55), 432 ($M^{\bullet+}$; 100), 431 (19), 430 (16), 417 ($[M - Me]^+$; 5), 360 (6), 359 ($[M - SiMe_3]^+$; 15), 357 (6), 355 (6), 287 ($[M - SiMe_3 - SiMe_2CH_2]^+$; 6), 73 (15). ^1H NMR (C_6D_6): δ 0.14 (s, 9H, C(1)Si*Me*$_3$); 0.33 (s, 9H, C(6)Si*Me*$_3$); 1.03, 1.14 (2 × d, $^2J_{HH} = 4.2$ Hz, 2 × 1H, C(2)=C*H*$_2$); 1.05 (s, 3H, C(4)*Me*); 1.11 (s, 2H, C(3)=C*H*$_2$); 1.47, 1.65 (2 × s, 2 × 3H, C(8)*Me* and C(9)*Me*); 1.53 (s, 3H, C(5)*Me*); 1.93, 2.01 (2 × s, 2 × 3H, C(7)*Me* and C(10)*Me*). $^{13}C\{^1H\}$ NMR (C_6D_6, 75 Hz): δ 1.91, 2.41 (C(1)Si*Me*$_3$ and C(6)Si*Me*$_3$); 10.58 (C(4)-*Me*); 11.23, 11.94 (C(8)*Me* and C(9)*Me*); 13.72 (C(5)*Me*); 15.24, 15.92 (C(7)*Me* and C(10)*Me*); 70.38 (C(3)=*C*H$_2$); 71.88 (C(2)=*C*H$_2$); 114.36 (*C*(6)); 119.11 (*C*(1)); 123.02, 123.31 (*C*(8) and *C*(9)); 127.29 (*C*(4)); 127.50, 127.85 (*C*(7) and *C*(10)); 143.87 (*C*(5)); 147.76 (*C*(2)); 148.88 (*C*(3)). $^{29}Si\{^1H\}$ NMR (C_6D_6): δ −7.59, −6.56 (C(1)*Si*Me$_3$ and C(6)*Si*Me$_3$). The carbon atoms are labeled in Chart 2. IR (KBr, cm^{-1}): 3050 (w), 2955 (s), 2907 (s), 2858 (m), 2730 (vw), 1481 (w), 1446 (m), 1403 (w), 1379 (m), 1335 (s), 1245 (vs), 1134 (w), 1026 (m), 891 (w), 835 (vs,b), 753 (s), 721 (w), 688 (m), 632 (m), 614 (w), 582 (w), 572 (vw), 446 (m). UV−vis (hexane, nm): 305 (sh) > 370 (sh) ≫ 585. Anal. Calcd for $C_{24}H_{40}Si_2Ti$ (432.63): C, 66.63; H, 9.32. Found C, 66.58; H, 9.30.

Chart 2

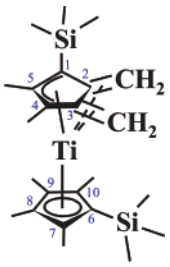

The gas formed during thermolysis was collected in a degassed charcoal cooled by liquid nitrogen. The trapped gas was evolved by warming to ambient temperature and collected in a sampling vessel. The EI MS analysis revealed the presence of hydrogen only.

Preparation of 3 by Thermolysis of $[Ti(\eta^2\text{-btmse})\{\eta^5\text{-}C_5Me_4(SiMe_3)\}_2]$ (2). Compound **2** (0.73 g, 1.21 mmol) was dissolved in 10 mL of toluene, and the solution was transferred into a distillation ampule on a vacuum line. After evaporation of toluene the ampule was successively heated to 150 °C. A blue oily solid containing yellow spots of apparently **2** condensed on tubes at room temperature. The distillate was dissolved in toluene, and the distillation was repeated. Then, the product was a blue wax crystallizing at room temperature. This was washed with hexane and crystallized as above. The yield of blue crystalline **3** was 0.24 g (72%). ^1H, ^{13}C, and ^{29}Si NMR spectra and EI-MS spectra proved the product to be identical with **3**.

During the first thermolysis all of the volatiles except hydrogen were trapped in a U-tube cooled by liquid nitrogen. GC MS analysis of this product revealed that it was btmse containing only about 0.1% of 1,2-bis(trimethylsilyl)ethene.

Thermolysis of the Titanocene 1 in Toluene Solution. Compound **1** (0.12 g, 0.276 mmol) in 10 mL of toluene was sealed in an evacuated ampule attached to a quartz cell and subsequently heated in a thermostated oven. No change in the electronic absorption spectrum was observed after heating to 110 °C for 8 h. However, the presence of a minute amount of evolved hydrogen was indicated after heating to 100 °C for 8 h by a slower distillation of the solvent upon cooling a wall of the vessel. After heating was carried out at 140 °C, the presence of gaseous hydrogen prevented the solvent distillation. It was also not possible to determine the content of **1** and **3** because of the proximity of their absorption band maxima (**1**, 570 nm; **3**, 585 nm). However, when the solution was cooled to ca. −20 °C, a new absorption band at 510 nm occurred and the band of **3** at 585 nm became quite discernible. This spectral change was reversible with the temperature. The absorption band at 510 nm has been attributed to an ochre titanocene−hydrogen complex which is stable only at low temperature.[27] The reasons for the less efficient thermolysis of **1** in solution are under investigation.

(26) Antropiusová, H.; Dosedlová, A.; Hanuš, V.; Mach, K. *Transition Met. Chem.* **1981**, *6*, 90−93.

(27) An ocher adduct of **1** with hydrogen characterized by λ_{max} 510 nm has been assigned to a titanocene complex with molecular hydrogen (tentatively **1**·$\mathbf{H_2}$) because its formation at low partial hydrogen pressure (<50 Torr) is observed at temperatures lower than −20 °C, and the complex reversibly dissociates into its components with increasing temperature. Mach, K. Unpublished results.

Thermolysis of the Titanocene [$Ti^{II}\{\eta^5$-$C_5Me_4(SiMe_2{}^iPr)\}_2$] (1A). The titanocene **1A**[12d] (0.43 g, 0.88 mmol) was dissolved in toluene, and the solution was transferred to a sublimation ampule and evaporated under vacuum with successive heating up to 150 °C. The thermolysis of the product collected on the tube wall at room temperature was repeated, and the product workup was carried out as above for obtaining **3**. The yield of blue waxy **3A** was 0.36 g (84%). EI-MS (110 °C): *m*/*z* (relative abundance) 492 (8), 491 (16), 490 (41), 489 (50), 488 ($M^{\bullet+}$; 100), 487 (16), 486 (14), 101 ($[SiMe_2{}^iPr]^+$; 5), 73 ($[SiMe_3]^+$; 14), 59 ($[SiMe_2H]^+$; 11). ^{1}H NMR (C_6D_6, 300 MHz): δ −0.05, 0.03 (2 × s, 2 × 3H, C(1)Si*Me*$_2$); 0.22, 0.25 (2 × s, 2 × 3H, C(6)Si*Me*$_2$); 1.01, 1.07 (2 × d, $^2J_{HH}$ = 3.6 Hz, 2 × 1H, C(2)=C*H*$_2$); 1.05 (s, 3H, C(4)*Me*); 1.10 (s, 2H, C(3)=C*H*$_2$); 1.14−1.26 (m, 14H, CH*Me*$_2$ and C*H*Me$_2$); 1.49, 1.67 (2 × s, 2 × 3H, C(8)*Me* and C(9)*Me*); 1.55 (s, 3H, C(5)-*Me*); 1.90, 2.05 (2 × s, 2 × 3H, C(7)*Me* and C(10)*Me*). ^{13}C{^{1}H} NMR (C_6D_6, 75 Hz): δ −2.44, −1.67 (C(1)Si*Me*$_2$); −1.48, −1.38 (C(6)Si*Me*$_2$); 10.64 (C(4)*Me*); 11.31, 12.10 (C(8)*Me* and C(9)*Me*); 13.90 (C(5)*Me*); 15.29, 16.12 (C(7)*Me* and C(10)*Me*); 15.90, 16.82 (*C*HMe$_2$); 18.20, 18.26 (C(1)SiMe$_2$(CH*Me*$_2$)); 18.38 (C(6)SiMe$_2$-(CH*Me*$_2$)); 70.22 (C(3)=*C*H$_2$); 72.24 (C(2)=*C*H$_2$); 113.11 (*C*(6)); 117.00 (*C*(1)); 123.28 (*C*(8) and *C*(9)); 127.34 (*C*(4)); 127.48, 128.70 (*C*(7) and *C*(10)); 144.07 (*C*(5)); 148.16 (*C*(2)); 148.85 (*C*(3)). ^{29}Si{^{1}H} NMR (C_6D_6): δ −2.50, −0.74 (C(1)*Si*Me$_2$ and C(6)*Si*Me$_2$). The carbon atoms are labeled as in Chart 2. IR (KBr, cm^{-1}): 3053 (vw), 2953 (vs), 2935 (s), 2914 (s), 2890 (m), 2861 (vs), 1462 (m), 1412 (w), 1380 (m), 1361 (w), 1331 (s), 1248 (vs), 1128 (w), 1070 (vw), 1022 (m), 999 (m), 918 (vw), 882 (m), 832 (s), 807 (vs), 764 (s), 679 (m), 592 (m), 571 (w), 424 (s). UV−vis (hexane): 585 nm.

Preparation of [TiMe$\{\eta^5$-$C_5Me_4(SiMe_3)\}_2$] (5). Crystalline [TiCl$\{\eta^5$-$C_5Me_4(SiMe_3)\}_2$] (0.7 g, 1.5 mmol) was dissolved in 40 mL of hexane, and the solution was poured over solid LiMe made by vacuum evaporation of its diethyl ether solution (2.0 mL, 1.9 M). The blue color of the monochloride turned rapidly to the green color of the methyl complex; however, the mixture was shaken for an additional 1 h to ensure the complete metathesis. Then, the green solution was poured away from a white solid and was cooled to −18 °C overnight. A clear solution was separated from a small amount of a white layer collected on the ampule walls. The volume of the solution was reduced to ca. 3 mL by distilling under vacuum, and the concentrated solution was cooled to −28 °C for 2 days. Dark green crystalline **5** was separated from the green mother liquor and dried under vacuum. Yield: 0.55 g (82%).

Data for **5** are as follows. Mp: 90−95 °C dec. EI-MS (70 °C): *m*/*z* (relative abundance) 449 ($M^{\bullet+}$; 5), 448 (6), 447 (7), 437 (11), 436 (35), 435 (69), 434 ($[M - Me]^+$; 100), 433 (48), 432 (21), 377 (7), 376 ($[M - SiMe_2]^+$; 17), 361 ($[M - SiMe_3]^+$; 7), 287 ($[M - Me - 2\ SiMe_3 - H]^+$; 8), 73 (18). IR (KBr, cm^{-1}): 2951 (s), 2905 (s), 2862 (m), 1481 (w), 1451 (w), 1404 (w), 1379 (m), 1348 (m), 1333 (s), 1247 (vs), 1127 (w), 1086 (vw), 993 (vw), 948 (vw), 1024 (m), 835 (vs, b), 755 (m), 688 (w), 632 (m), 575 (vw), 422 (m). ESR (hexane, 22 °C): g = 1.956, ΔH = 13 G. ESR (toluene, −140 °C): g_1 = 1.999, g_2 = 1.982, g_3 = 1.888, g_{av} = 1.957. UV−vis (hexane, 22 °C): 460 > 595 nm. Anal. Calcd for $C_{25}H_{45}Si_2Ti$ (449.69): C, 66.77; H, 10.09. Found: C, 66.71; H, 9.99.

Thermolysis of 5 To Give [Ti$\{\eta^5$-$C_5Me_4(SiMe_3)\}\{\eta^5$:$\eta^1$-$C_5Me_4$-$(SiMe_2CH_2)\}$] (4). Compound **5** (0.4 g, 0.9 mmol) was dissolved in toluene (10 mL), and the solution in a sealed ampule (100 mL volume) was heated to 130 °C for 2 h. The ampule was opened to a vacuum line, and after a sample of gas was collected for GC-MS analysis all volatiles were evaporated under vacuum. A dark green residue was dissolved in hexane and crystallized from 2.0 mL of the solution by cooling to −28 °C. After 2 days, a dark green crystalline solid was isolated from the mother liquor and dried under vacuum. The yield of **4** was 0.33 g (85%). All spectroscopic data agreed with those reported for **4**, and a single-crystal X-ray diffraction study determined the same unit cell parameters.[7]

Data for **4** are as follows. Mp: 125 °C. EI-MS (90 °C): *m*/*z* (relative abundance) 436 (10), 435 (35), 434 (69), 433 ($M^{\bullet+}$; 100), 432 (30), 431 (27), 430 (6), 429 (18), 418 ($[M - Me]^+$; 11), 362 (7), 361 (19), 360 ($[M - SiMe_3]^+$; 11), 287 ($[M - 2\ SiMe_3]^+$; 7), 73 ($[SiMe_3]^+$; 21). IR (KBr, cm^{-1}): 2968 (s), 2950 (vs), 2906 (vs), 2863 (s), 1481 (w), 1448 (m), 1405 (w), 1378 (s), 1347 (m), 1329 (s), 1246 (vs), 1128 (w), 1084 (vw), 1022 (s), 993 (vw), 948 (vw), 843 (vs, b), 788 (s), 758 (s), 685 (m), 670 (s), 642 (m), 634 (m), 572 (vw), 520 (w), 469 (s), 429 (s). EPR (toluene, 23 °C): g = 1.959, ΔH = 15 G. UV−vis (hexane, 22 °C): 320 (sh) > 375 (sh) > 460 > 600 nm. GC MS analysis of the gaseous sample: methane-[tmt]toluene.

Preparation of [TiMe$_2\{\eta^5$-$C_5Me_4(SiMe_3)\}_2$] (6). A slurry of [TiCl$_2\{\eta^5$-$C_5Me_4(SiMe_3)\}_2$] (1.0 g, 2.0 mmol) in hexane (50 mL) was transferred onto dry LiMe isolated from its solution in diethyl ether (1.9 M, 4.0 mL, 7.6 mmol) by evaporation under vacuum at 70 °C. The mixture was shaken for 1 h at 40 °C. After sedimentation of a yellowish slurry, a clean orange-yellow solution was separated, the solvent was distilled back onto the slurry, and the second extract was added to the first one. The combined extracts were cooled to −5 °C overnight, which caused the precipitation of a yellowish solid layer on the ampule walls. The bright orange-yellow solution was transferred to another ampule, the solvent was mostly distilled off, and the concentrated solution was cooled in a freezer to −30 °C overnight. Orange needlelike crystals were separated from the mother liquor, washed with cool hexane, and dried under vacuum. Yield: 0.81 g (87%).

Data for **6** are as follows. Mp: decomposition, at 104 °C yellow crystals disintegrated, at 118−120 °C melting with gas evolution. ^{1}H NMR (C_6D_6): δ −0.23 (s, 6H, Ti*Me*$_2$); 0.32 (s, 18H, Si*Me*$_3$); 1.60 (s, 12H, C$_5$*Me*$_4$); 2.10 (s, 12H, C$_5$*Me*$_4$). ^{13}C{^{1}H} NMR (C_6D_6): δ 2.51 (Si*Me*$_3$); 12.06, 15.57 (C$_5$*Me*$_4$); 50.02 (Ti*Me*$_2$); 120.68 (C_{ipso}); 123.73, the second is overlapped by solvent signal (C_q; C_5Me_4). ^{29}Si{^{1}H} NMR (C_6D_6): δ −7.03 (*Si*Me$_3$). EI MS (110 °C): *m*/*z* (relative abundance, %) 464 ($M^{\bullet+}$, not observed), 450 (8), 449 (16), 448 ($[M - CH_4]^+$; 22), 447 (17), 437 (8), 436 (23), 435 (47), 434 ($[M - 2\ Me]^+$; 100), 433 (77), 432 (20), 431 (10), 378 (8), 377 (15), 376 ($[M - 2\ Me - SiMe_2]^+$; 35), 375 (13), 361 ($[M - 2\ Me - SiMe_3]^+$; 8), 287 (11), 285 (9), 283 (10), 242 (10), 241 (19), 240 ($[M - 2\ Me - Cp'H]^+$; 74), 239 (33), 238 (12), 225 (8), 224 (20), 223 (14), 222 (18), 221 (19), 220 (13), 219 (10), 218 (10), 217 (11), 208 (12), 207 (12), 206 (10), 167 (13), 73 ($[SiMe_3]^+$; 76), 59 ($[SiMe_2H]^+$; 15). IR (KBr, cm^{-1}): 2976 (s), 2957 (s), 2901 (s), 1485 (w), 1452 (w), 1433 (w), 1409 (w), 1379 (m), 1342 (m), 1332 (m), 1246 (s), 1126 (w), 1084 (vw), 1022 (m), 841 (vs,b), 756 (m), 685 (w), 637 (w), 450 (w), 414 (m). UV−vis (hexane): 423 nm. Anal. Calcd for $C_{26}H_{48}Si_2Ti$ (464.72): C, 67.20; H, 10.41. Found: C, 67.16; H, 10.37.

Preparation of [Ti$\{\eta^6$:η^1-$C_5Me_3(CH_2)(SiMe_2CH_2)\}\{\eta^5$-$C_5Me_4$-$(SiMe_3)\}$] (7). Compound **6** (0.5 g, 1.08 mmol) was dissolved in 20 mL of toluene, and the obtained solution was heated in a sealed ampule (volume 100 mL) to 102 °C for 8 h. After the mixture was cooled to ambient temperature, all volatiles were distilled off (a sample of gaseous products was collected), and the green residue was extracted with hexane (3.0 mL). Cooling to −28 °C in a freezer for 3 days afforded turquoise crystalline **7**. Yield: 0.35 g (76%).

Data for **7** are as follows. Mp: 105 °C. ^{1}H NMR (C_6D_6): δ −3.95, −0.57 (2 × d, 2 × $^2J_{HH}$ = 12.9 Hz, 2 × 1H, TiC*H*$_2$Si); 0.16 (s, 9H, Si*Me*$_3$); 0.33, 0.47 (2 × s, 2 × 3H, CH$_2$Si*Me*$_2$); 1.12 (s, 3H, C(3)*Me*); 1.15 (partially overlapped by a stronger methyl signal, 1H, TiC*H*$_2$); 1.30, 1.76 (2 × s, 2 × 3H, C(8)*Me* and C(9)-*Me*); 1.58 (s, 3H, C(4)*Me*); 1.64, 2.17 (2 × s, 2 × 3H, C(7)*Me* and C(10)*Me*); 2.04 (s, 3H, C(5)*Me*); 2.06 (partially overlapped by a stronger methyl signal, 1H, TiC*H*$_2$). ^{13}C{^{1}H} NMR (C_6D_6): δ 0.65, 6.23 (CH$_2$Si*Me*$_2$); 2.25 (Si*Me*$_3$); 10.38, 11.24, 11.98, 12.07, 14.24,

Chart 3

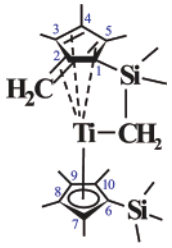

15.01, 16.19 (C_5Me_4 and C_5Me_3); 37.48 (TiCH_2Si); 77.14 (TiCH_2); 111.20 (*C*(6)); 119.87, 123.79 (*C*(8) and *C*(9)); 120.25 (*C*(1)); 128.18, 131.99 (*C*(7) and *C*(10)); 130.25 (*C*(3)); 131.73 (*C*(5)); 134.58 (*C*(4)); 134.66 (*C*(2)). ^{29}Si{^{1}H} NMR (C_6D_6): −8.04, −7.79 (CH_2SiMe_2 and $SiMe_3$). The carbon atoms are labeled in Chart 3. EI MS (110 °C): *m*/*z* (relative abundance, %) 435 (8), 434 (27), 433 (52), 432 ($M^{\bullet+}$; 100), 431 (34), 430 (54), 429 (14), 428 (12), 359 ($[M - SiMe_3]^+$; 14), 358 (9), 357 (20), 356 (11), 355 (23), 354 (10), 353 (17), 352 (7), 351 (12), 218 (10), 217 (12), 73 ($[SiMe_3]^+$; 90). IR (KBr, cm^{-1}): 3062 (vw), 2953 (s), 2903 (s), 2860 (sh), 1486 (w), 1445 (m, b), 1404 (m), 1379 (s), 1360 (w), 1349 (m), 1331 (s), 1312 (m), 1247 (vs), 1137 (m), 1131 (m), 1088 (vw), 1019 (s), 948 (vw), 847 (vs, b), 756 (s), 687 (m), 649 (s), 632 (m), 612 (vw), 575 (vw), 522 (w), 470 (w), 427 (m). UV−vis (toluene): 624 nm. Anal. Calcd for $C_{24}H_{40}Si_2Ti$ (432.63): C, 66.63; H, 9.32. Found: C, 66.58; H, 9.29.

X-ray Crystallography. A blue prism of **3** and green fragments of **5** and **7** were mounted into Lindemann glass capillaries in a Labmaster 130 glovebox (mBraun) under purified nitrogen. The diffraction data for complex **3** were collected on a Nonius KappaCCD image plate diffractometer (Mo Kα radiation, λ = 0.710 73 Å) and analyzed by the HKL program package.[28] The data for **5** were collected on a CCD Xcalibur S diffractometer and those for **7** on a Siemens CCD SMART diffractometer (Mo Kα radiation, λ = 0.710 73 Å) using φ-scan rotation. The structures were solved by direct methods (SIR97),[29] followed by consecutive Fourier syntheses and refined by full-matrix least squares on F^2 (SHELX97).[30] All non-hydrogen atoms were refined anisotropically. Hydrogen atoms were included in ideal positions and refined isotropically using the riding model, except for hydrogen atoms on the exo methylene groups of **3**. These were found on a difference Fourier electron density map and refined isotropically without any restraints. Crystallographic data and data collection and structure refinement details for **3**, **5**, and **7** are given in Table 4.

Computational Details. DFT calculations have been performed at the Supercomputer Centre of Charles University using Gaussian 98, Revision A.7 (G98-A.7)[31] and at the Computer Centre of the J. Heyrovský Institute of Physical Chemistry using Gaussian 03, Revision B.05 (G03-B.05).[32] UV−vis transitions for **1** and **3** were determined by time-dependent DFT (TD) and NMR shielding constants using GIAO's, both as implemented in Gaussian. Since **1**, **3**, and **7** were processed on computers with different performances and loads, their treatments were different and are summarized below.

1: G03-B.05; geometry optimization, spin-unrestricted BPW91/6-311G(d,p), Hessian computed analytically; point group C_{2h} of the solid-state structure was retained; TD, spin-unrestricted BPW91/6-311+G(3d,p), Douglas−Kroll−Hess second-order scalar relativistic Hamiltonian, ultrafine integration grid.

3: G98-A.7; geometry optimization, BPW91/6-311G, approximate Hessian, ultrafine integration grid; TD, B3LYP/6-311G(2d), ECP[33] on Ti, Douglas−Kroll−Hess second-order scalar relativistic Hamiltonian, ultrafine integration grid.

7: G03-B.05; geometry optimization, B3LYP functional, 6-311+G(d,p) basis set on the Ti atom and all atoms in the Si-CH2 moiety, other atoms 6-311G, Hessian computed analytically; GIAO shielding, B3LYP functional; ECP[33] on Ti; 6-311++G(3d,p) on other atoms, ultrafine integration grid.

Orbital numberings in the text are the same as from Gaussian. Contours of all molecular orbitals, including the section of orbital 113 of **1**, were obtained using Molden.[34]

Table 4. Crystallographic Data and Data Collection and Structure Refinement Details for 3, 5, and 7

	3	**5**	**7**
formula	$C_{24}H_{40}Si_2Ti$	$C_{25}H_{45}Si_2Ti$	$C_{24}H_{40}Si_2Ti$
M_r	432.64	449.69	432.64
cryst syst	orthorhombic	triclinic	triclinic
space group	*Pbcn* (No. 60)	$P\bar{1}$ (No. 2)	$P\bar{1}$ (No. 2)
a (Å)	33.5080(2)	8.5124(10)	9.080(6)
b (Å)	12.1320(2)	9.0457(15)	9.583(7)
c (Å)	12.3750(6)	19.055(3)	14.339(10)
α (deg)	90.00	95.941(14)	80.987(12)
β (deg)	90.00	91.303(12)	82.538(12)
γ (deg)	90.00	114.724(13)	89.766(13)
V (Å^3); Z	5030.7(3); 8	1356.0(4); 2	1221.7(15); 2
T (K)	150(2)	150(2)	223(2)
Z	8	2	2
D_{calcd} (g cm^{-3})	1.142	1.130	1.176
μ (mm$^{[1]}$)	0.442	0.423	0.455
color; habit	blue, prism	dark green, prism	dark green, prism
cryst dimens (mm^3)	0.40 × 0.25 × 0.25	0.78 × 0.64 × 0.19	0.20 × 0.10 × 0.10
no. of diffrns collected	54494	41386	6816
θ range (deg)	1.22−27.49	2.78−30.51	2.15−23.48
hkl range	−43 to +43; −15 to +15; −16 to +16	−12 to +12; −12 to +12; −27 to +27	−9 to +10; −10 to +10; −16 to +15
no. of unique diffrns	5766	7993	3385
no. of obsd diffrns, $I > 2\sigma(I)$	4839	7993	2266
F(000)	1872	490	468
no. of params	272	422	244
$R(F)$; $R_w(F^2)$ (%)	4.97; 9.60	5.42; 10.70	17.99; 39.98
GOF(F^2), all data	1.080	1.193	1.141
$R(F)$; $R_w(F^2)$ ($I > 2\sigma(I)$)	3.88; 9.12	4.36; 10.10	13.86; 38.03
$\Delta\rho$ (e Å^{-3})	0.569; −0.394	0.586; −0.305	1.666; −0.695

Acknowledgment. This research was supported by the Grant Agency of the Czech Republic (Grant No. 104/05/0474). R.G. and I.C. thank MSM0021620857.

Supporting Information Available: CIF files for the structures of **3**, **5**, and **7**, tables, figures, and text giving additional details of the X-ray structures of **3**, **5**, and **7** and a discussion of the crystal structure of **3**, and tables and figures giving computational details for titanocene **1** and compounds **3** and **7**, frontier molecular orbital energies and graphical representations of the orbitals, calculations of UV−vis spectra for **1** and **3**, and calculations of NMR spectra for **7** and their correlation with experimental data. This material is available free of charge via the Internet at http://pubs.acs.org.

OM070159L

(28) Otwinowski, Z.; Minor, W. HKL Denzo and Scalepack Program Package; Nonius BV, Delft, The Netherlands, 1997. For a reference see: Otwinowski, Z.; Minor, W. *Methods Enzymol.* **1997**, *276*, 307−326.

(29) Altomare, A.; Burla, M. C.; Camalli, M.; Cascarano, G.; Giacovazzo, C.; Guagliardi, A.; Polidori, G. *J. Appl. Crystallogr.* **1994**, *27*, 435−436.

(30) Sheldrick, G. M. SHELXL97: Program for Crystal Structure Refinement from Diffraction Data; University of Gottingen, Gottingen, Germany, 1997.

(31) Frisch, M. J. et al. *Gaussian 98*, revision A.7; Gaussian, Inc.; Pittsburgh, PA, 1998 (see the full reference in the Supporting Information).

(32) Frisch, M. J. et al. *Gaussian 03*, revision B.05; Gaussian, Inc.; Wallingford, CT, 2004 (see the full reference in the Supporting Information).

(33) Hurley, M. M.; Pacios, L. F.; Christiansen, P. A.; Ross, R. B.; Ermler, W. C. *J. Chem. Phys.* **1986**, *84*, 6840−6853.

(34) Schaftenaar, G.; Noordik, J. H. Molden: a pre- and postprocessing program for molecular and electronic structures. *J. Comput.-Aided Mol. Des.* **2000**, *14*, 123−134.